Proc. QENS/WINS 2012
J. Phys. Soc. Jpn. **82** (2013) SA011

Quasi-Elastic Neutron Scattering Study of Water Confined in Periodic Mesoporous Organosilicas

Dehong Yu[1], Daniel Page[1], Jichen Li[2], Yitzhak Mastau [3], Michael Koza[4] and Gordon Kearley[1]

[1]*Bragg Institute, Australian Nuclear Science and Technology Organization, New Illawarra Road, Lucas Heights, 2234, Australia*
[2]*School of Physics and Astronomy, University of Manchester, Oxford Road, M13 9PL Manchester, UK.*
[3]*Department of Chemistry and the Institute of Nanotechnology, Bar-Ilan University, Ramat-Gan, 52900 Israel.*
[4]*Institut Laue Langevin, 6 rue Jules Horowitz, BP156, F-38042 Grenoble, France*

E-mail: dyu@ansto.gov.au
(Received December 18, 2012)

Water confined in nanoscale space behaves significantly differently from bulk water. We have applied the Quasi-Elastic Neutron Scattering technique to investigate diffusive properties of water confined in porous silicate coated with hydrophobic organic functional groups, at two different levels of hydration. The measurements were performed over a wide range of temperatures, and although we cannot exclude subdiffusion, the data are more easily understood from a distribution in the diffusive dynamics ranging from static water monolayer at the pore surface to much greater mobility towards the pore centre. There is some evidence for a local diffusive motion with an effective radius of about 3.5 Å. The overall diffusion constants are significantly less than bulk water over the same temperature ranges.

KEYWORDS: water, QENS, porous silicate

1. Introduction

Water is an excellent solvent for many biological systems, and understanding its structure and dynamics in different situations is of great importance [1]. Over recent years, the dynamical and structural properties of water in confined spaces, such as in pores of porous media, has drawn considerable interest, due to the importance in both providing fundamental understanding of biological systems and solving technological problems such as oil recovery from natural reservoirs, mining, function of membranes and enzymatic activity [2,3].

The structural and dynamical properties of bulk water are already well-known under many circumstances [4], and the behaviour of supercooled water has recently been substantially re-examined using quasielastic neutron scattering (QENS) [5]. It is well known that the exceptional chemical and physical properties of water come from the bonds that water molecules form with their neighbours, especially via hydrogen bonds [2].

However, in many common situations, water is attached to a surface, either hydrophilic or hydrophobic, or fills in small cavities, rather than being simply in its bulk form. The behaviour of this interfacial or confined water is quite different from that of bulk water, due to the structural perturbations from confinement and interactions with surfaces [3].

The water motion can be significantly slowed down by nano-scale confinement. The slow-down of water dynamics was observed in Vycor porous glass [6], ordered mesoporous silica of MCM-41 with various pore sizes [7,8,9,10], SBA-15 and mesoporous alumina [11]. For these materials, interfacial water is usually formed at the hydrophilic pore surface and the water dynamics are mainly governed by the strong interaction of water with the pore surface. The motion of water can be slowed down by a factor of five [12]. The dynamic behaviour of the interfacial water is similar to the bulk supercooled water at lower temperature [13, 14]. For materials with hydrophobic pore surface, like carbon nanotubes, the water dynamics are expected to be different from the hydrophilic cases. Through molecular dynamic simulation (MD), Hummer *et al* [15] predicated pulse-like transmission of water through carbon nanotubes (CN) and possible enhancement of water motion as a result of much less interaction with the hydrophobic wall. Several QENS studies of water confined inside carbon nanotubes [16,17,18] have observed a much lower dynamic crossover (fragile-to-strong) temperature as compared with materials having hydrophilic pore surface. However, these experiments have shown that the water diffusion property in CN is actually similar to that of water confined in other porous materials with hydrophilic surface.

To shed more light on these issues, we present an initial study using QENS to investigate the main dynamical characteristics of water confined in periodic mesoporous organosilicas (PMOs) based on hydrophobic phenyltriethoxysilane (PTES) with the aim of establishing a model system for more detailed analysis of pore-surface effects, specifically, for system having hydrophobic pore surface. Diffusive properties of water in PTES silica gel with 30% water by weight (silica30) and 60% water by weight (silica60) were investigated.

2. Experiment and Data Analysis

2.1 Synthesis of PTES

Inorganic-organic mesoporous silica was synthesized at room temperature from mixtures containing a constant molar ratio of a functionalized organotrialkoxysilane with tetraethoxysilane (TEOS) in the presence of the surfactant C_{16}TAB. For the synthesis of the periodic mesoporous organosilicas, a solution composed of molar ratio: Si : C_{16}TAB : H_2O : NH_4OH of 1.0 : 0.12 : 130.1 : 0.5 was prepared. Typically, a solution was made of water (2.34 ml 0.13mol) ammonium hydroxide (0.02 g, 0.5 mmol) and C_{16}TAB (0.044 g, 0.12 mmol). The surfactant was dissolved by warming the solution to 40°C. Then, a mixture containing a constant molar ratio of PTES (0.048 g, 0.2 mmol) with TEOS (0.17 g, 0.8 mmol) was added drop wise to this solution with rapid stirring. PTES and TEOS were mixed before addition to the surfactant solution. Once the solution had homogenized, the stirring was slowed for an additional 10 min. After aging at 80 °C for 4 days, the product was isolated by filtration as a white powder. The surfactant template was removed from the organosilica materials through solvent extraction process. A 2 g sample of product was refluxed in 3 mL of (37 wt. %) HCl/200ml of methanol for 1 day, collected by suction filtration, washed with water and dried in air at room temperature.

2.2 Sample Characterization

Small-Angle X-Ray Scattering (SAXS) and High Resolution Transmission electron microscopy (HR-TEM) have been applied in the characterization of the sample. SAXS has shown that the synthesized material has a two-dimensional hexagonal lattice structure (space group p6mm). The HR-TEM has clearly revealed that the material has a highly porous "wormhole structure" with disordered pores with an averaged pore size of around 40 Å. FT-IR spectroscopy on PTES sample revealed several typical absorption bands of the incorporated organic group, such as, aromatic ring C-C stretches at 1591 cm^{-1}; C – H bends at 740 and 700 cm^{-1} and the most typical and important band of aromatic C-Si stretch at 1430 cm^{-1}. These results confirmed that our sample is a true organosilica with the incorporation of the organic-inorganic precursors.

2.3 Quasi-Elastic Neutron Scattering (QENS)

The QENS experiment was performed at the Institute Laue-Langevin (ILL) in Grenoble, France, using the cold neutron time-of-flight spectrometer IN6. The neutron wavelength of 5.1 Å was used and momentum transfer range from 0.25 $Å^{-1}$ to 2 $Å^{-1}$ was covered. Data reduction using LAMP (http://www/ill/fr/data_treat/lamp/lamp.html) converts the measured differential cross section to experimental $S_{inc}(Q,\omega)$ with regular Q and energy interval. The data reduction procedure took account of background subtraction, sample geometry correction and normalization to vanadium data.

2.4 Theoretical Background

Due to the large incoherent cross section of hydrogen in the samples the measured differential cross section is approximately given by [19]:

$$\frac{d^2\sigma}{dEd\Omega} = \frac{\sigma_{inc}}{4\pi}\frac{k_s}{k_i} NS_{inc}(Q,\omega) \tag{1}$$

The conservation of the momentum and energy during the scattering process gives

$$\hbar\vec{Q} = \hbar(\vec{k}_s - \vec{k}_i), \quad \hbar\omega = E - E_0 \tag{2}$$

where σ_{inc} is the total incoherent cross section, E_0, E, $\vec{k}_i$ and $\vec{k}_s$ are the neutron energy and wave vectors before and after the scattering and $\vec{Q}$ is the scattering vector. N is the number of scatters, $\hbar\vec{Q}$ and $\hbar\omega$ is the momentum and energy transfer, respectively. $S_{inc}(Q,\omega)$ is the incoherent dynamic structure factor containing the full information about the dynamical process.

Theoretically, the incoherent dynamic structure factor can be expressed as the convolution among vibrational, translational and rotational motions:

$$S_{inc}^{theory}(Q,\omega) = S_V(Q,\omega) \otimes S_T(Q,\omega) \otimes S_R(Q,\omega) \tag{3}$$

In the QENS domain, the vibrational motion can be approximately described by the Debye-Waller (DW) factor [19]

$$S_V(Q,\omega) = DW = \exp\left(-\tfrac{1}{3}Q^2\left\langle u^2\right\rangle\right) \tag{4}$$

where $\left\langle u^2\right\rangle$ is the mean square vibrational displacement of hydrogen atoms.

The rotational motion is usually much faster than the translational motion and thus can either contribute as a background or as a broad feature under the dominant component of the translational motion in the current experimental resolution window.

This leads to the following approximation for the experimental incoherent dynamic structure factor:

$$\begin{aligned} S_{inc}(Q,\omega) &= S_{inc}^{theory}(Q,\omega)\otimes R(Q,\omega) \\ &= \exp\left(-\tfrac{1}{3}Q^2\left\langle \mu^2\right\rangle\right)S_T(Q,\omega)\otimes R(Q,\omega) \end{aligned} \tag{5}$$

where $R(Q,\omega)$ is the experimental resolution function .

Contributions to the $S_T(Q,\omega)$ term in eq. (5) can be from hydrogen atoms belong to different populations in the sample. The hydrogen atoms within the frame of silica and water confined in the pores within the silica can cause elastic scattering. The quasi-elastic scattering may come from the translational motion of water confined within the pore. The vibrational motion from all hydrogen atoms in the sample can be represented by the average Debye-Waller factor.

It is convenient to describe the probability that an atom remains within a certain volume, that is I(Q,∞), as the elastic incoherent structure factor (EISF). This is usually expressed as the elastic intensity divided by the total spectral intensity and the way in which the EISF varies with Q reflects the geometrical aspects of the diffusing particle.

2.5 Data Analysis

We have no atomistic-scale model for this system and we therefore need to find an analytical description of the data to understand the basic underlying dynamics of the water. Attempts to fit the data with an elastic peak plus a single Lorentzian function were entirely unsatisfactory, and following recent reports for QENS on water [5], we then used an elastic peak and two Lorentzian functions. This combination provided adequate fitting of the data but at low Q the width of the Lorentzian components increased with decreasing Q, which we considered unphysical. This is not to say that the model used in ref. 5 does not apply here, but that there are additional complexities in the present case.

QENS measures the decay of the initial particle state (in the present case H atoms) with time. A single exponential decay is reflected by a Lorentzian function in frequency domain in which experiment is performed. Although normal bulk water is often analysed as a single decay, in other environments two decay processes are observed, which may not be translation and rotation as previously proposed, but diffusion in clusters and between clusters as shown recently [5]. The poor fitting of the two Lorentzian functions in our case implies that no single or pair of decay processes can be derived and that some distribution may be needed to model the decay of H atoms in the time domain. It turns out that we get physically reasonable fits to our data using a simple distribution that invokes fewer parameters than the two-Lorentzian model above. The approach we used is common in these situations, which is empirical stretched exponential function or Kohlrausch-Williams-Watts (KWW) function [20]:

$$P(t) = f \exp[-(t/\tau)^{\beta}] \tag{6}$$

Here, P is the overall probability that the system is in the initial state, and τ is the effective relaxation time from the superposition of decay processes. β is a stretching parameter that decreases as the distribution of relaxation process increases. The amplitude parameter f is a measure of the fraction of the experimental quantity being investigated. The difficulty is that the KWW function does not provide unambiguous information of the underlying processes, but with the present system the most likely candidates are either subdiffusion in which barriers to mobility evolve with time, or a spatial distribution of barriers within the pores. We will make this distinction by considering the characteristics of the system and the QENS data.

Our experimental data are in the frequency domain and a convenient approximation for the stretched exponential in this domain is given by the following susceptibility Bergman function [20]:

$$X''(\omega) = X''_p \Bigg/ \left(1 - b + \frac{b}{1+b}\left[b\left(\frac{\omega_p}{\omega}\right) + \left(\frac{\omega}{\omega_p}\right)^b\right]\right) \tag{7}$$

where Xp'' is the maximum in the susceptibility, ω_p is a width parameter, and b is a shape parameter directly related to the stretching parameter, β, in eq. (6). Taking into account the elastic component, we constructed a global fitting procedure to fit the experimental data as a function of Q and ω simultaneously with the following function [21]:

$$S_{inc}(Q,\omega) = e^{-\frac{1}{3}Q^2\langle\mu^2\rangle}\left\{\left[X''_p \Bigg/ \left(\omega\left(1 - b + \frac{b}{1+b}\left[b\left(\frac{\omega_p}{\omega}\right) + \left(\frac{\omega}{\omega_p}\right)^b\right]\right)\right)\right] + (1 - X''_p)\delta_{ep}\right\} \otimes R(Q,\omega) \tag{8}$$

The first part of this function contains only three adjustable parameters: ω_p, b, and X_p'', which are given as independent of Q. δ_{ep} is a delta function representing the elastic peak contribution, the whole being convoluted with $R(Q,\omega)$, the measured experimental resolution function.

For the purpose of comparison, if b > 0.5 then b is analogous to β and ω_p to the width of an equivalent Lorentzian function. The parameters in eq. (8) are usually linked to the parameters of the stretched exponential decay of eq. (6) [20]:

$$b \approx \beta \tag{9a}$$

$$X''_p \approx \frac{f}{2}\beta \tag{9b}$$

$$\omega_p \approx 1 \Bigg/ \left(\tau\sqrt{\frac{1}{\beta}\Gamma\left(\frac{1}{\beta}\right)}\right) \tag{9c}$$

For each temperature, nine experimental spectra corresponding to different Q-values were available and attempts were made to find the best constraints with which to fit these spectra at different Q simultaneously. The best result was obtained by assuming that the total spectral intensity is constant, but reduced by a Debye-Waller factor, and distributed between the elastic and a single quasielastic component described by the Bergmann function. ω_p (width) of the Bergmann function was constrained to increase as Q^2, and the shape parameter b, was constrained to be constant with Q. We have not explicitly accounted the rotational motion in the fitting, but simply absorbed the possible contributions in the background and probably also part of the quaselastic tails. A proper analysis including rotational motions would require further measurements in a different time scale combined with molecular dynamic simulations.

Eq. (8) is basically the approximation of the relaxing cage model (RCM) [22] in the frequency domain. According to the RCM the translational dynamics of water is expressed as the product of a short-time harmonic motion and a long-time decay. The short-time harmonic motion represents the water motion inside a cage of its neighbours and it can be approximated by the Debye-Waller factor within QENS time scale. The long-time decay process models the structural relaxation of the cage which cannot be described by a simple Debye process (exponential decay) and is better described by a stretched exponential decay process. The RCM has been successfully applied in many cases like, supercooled water [23,24,25], porous silica [10, 26, 27], and carbon nanotubes and nanopores [16, 17].

2.6 Results and Discussions

The presence of an elastic peak provides an elastic incoherent structure factor (EISF) as a function of Q for silica60 and sillica30 which are displayed in Fig. 1 and 2, respectively, for different temperatures. The EISF decreases with increasing temperature without showing much change in profile. This suggests a population of water molecules that undergo a diffusive motion within a restricted volume which increases as the temperature is increased. Notwithstanding the role of small-angle scattering at low Q, it seems that there is probably a steep fall in the EISF at low Q. It would be unrealistic to propose a single process that accounts for the EISF, which is the resultant of a number of processes in the present case. Nevertheless, we note that there is consistently a flatter region between about 1.0 and 1.5 $Å^{-1}$ which shows that there is at least some resemblance to isotropic rotation. The general appearance of the EISF at high Q suggests that a fraction of the water molecules are static on the timescale of the instrument, and in order to obtain an estimate of this fraction we have adjusted the radius and static fraction of the EISF for spherical rotation to get some comparison with the experimental EISF. We obtained the solid line in figure 1 which is the EISF for spherical rotation of 80% of the H-atoms on a radius of 3.5Å, the remainder being static. Interestingly, for a 40Å diameter pore, the 20% immobile water corresponds closely to a monolayer at the surface of the pore, with the rest of the water presumably becoming more mobile as the centre of the pore is approached. This is also consistent with the EISF at high Q being almost twice as high for the silica30 than the silica60, reflecting that the quantity of immobile water is the same in both samples. We stress that the rotational diffusion model used for the EISF was chosen to get some approximation of distance and static fraction, and the fit clearly cannot support a simple rotational diffusion alone.

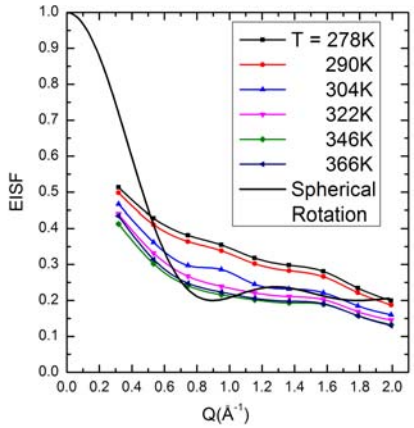

Fig. 1. EISF versus Q for Silica-60 sample at a variety of temperatures. The curve without symbols is for comparison with the EISF of spherical rotation on a radius of 3.5Å.

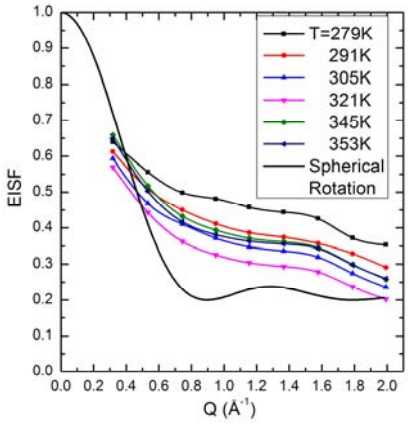

Fig. 2. EISF versus Q for Silica-30 sample at similar temperatures to figure 1. The EISF for spherical rotation on a radius of 3.5Å is shown for comparison.

To obtain more information we examine the dynamical information held in the QENS signal itself. We have only a rather qualitative picture of the diffusion process from the above so that we are limited to extracting an effective diffusion constant from ω_p of the Bergmann function. Using the simple Fick's law approach, the diffusion constant is obtained from the width that increases as DQ^2:

$$S(Q,\omega) = \frac{1}{\pi}\frac{DQ^2}{\omega^2+(DQ^2)^2} \tag{10}$$

corresponding to the slope of ω_p vs Q^2. The effective diffusion constants are illustrated in Fig. 3 as a function of temperature, together with the bulk water values reported recently [28]. These values are evidently much lower than those for bulk water over this temperature range. Further, the diffusion constants increase more slowly with temperature for the lower hydration of silica30, which is consistent with the water interacting with the pore, despite the pore surface being hydrophobic. For comparison, the water diffusion constants at temperatures around 300 K and 270 K are listed in table I for different systems. The current diffusion constants for both samples of silica30 and silica60 fall into the range of other systems of Vycor glass, porous silica and carbon nanotubes having different pore size and pore surface properties. It shows that the water mobility under confinement is about a factor of 2 slower than bulk water at similar temperatures. It seems that the size of the pore (1.2 nm to 5 nm) and the detail surface properties (hydrophilic or hydrophobic) play little role in determining the water diffusion property under nanoscale confinement, although the microscopic mechanism may be very different for these systems.

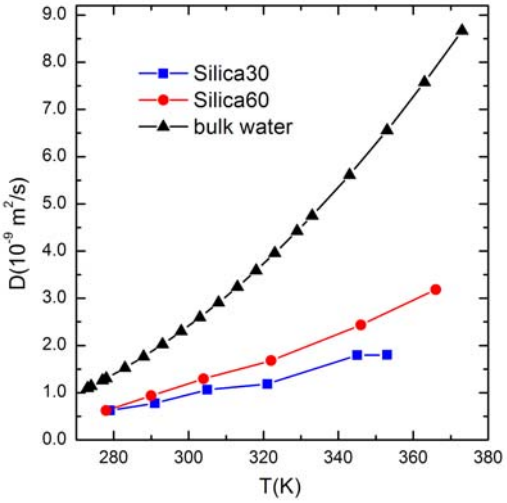

Fig. 3. The effective diffusion constant as a function of temperature for the two samples. Theses curves show a diffusion constants less than half that of bulk water, where these values are taken from reference [28].

Table I. Comparison of water diffusion constants, D, for different systems at temperatures around 300 K and 270 K.

Sample	Pore size (nm)	D ($10^{-9}m^2/s$)	T(K)	References
Sillica30	4	1.06	305	Present
		0.62	279	Present
Sillica60	4	1.29	304	Present
		0.62	278	Present
Vycor	5	1.1	293	23
	5	0.75	258	29
MCM41	2.14 – 2.84	1.07 – 1.45	298	10
		0.47	268	10
SWNT	1.4	0.54	260	18
DWNT	1.6	0.35	240	18
Bulk water		2.299	298	28
		1.099	273	28

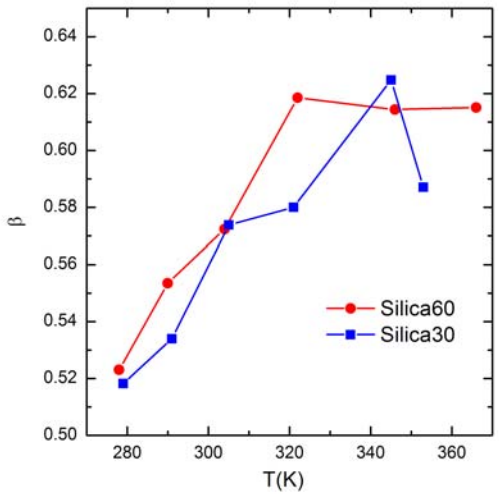

Fig. 4. The stretching parameters, β, as a function of temperature for the two samples. Values are similar for both samples.

Figure 4 shows that the β values are rather similar for the two hydrations, and increase with temperature. This suggests that the distribution of water mobilities is much the same for the two samples, and that this mobility becomes more homogenous as the

temperature is increased. Presumably, the water increasingly overcomes its interaction with the surface as its kinetic energy increases.

It turns out that it is not easy in this case to distinguish between subdiffusion or static inhomogeneity, or indeed a combination of these, as the origin of the stretched exponential decay. The stretching parameter, β, reflects the non-surface water and we see no significant difference for this, which might suggest that the difference between the samples is the number of filled pores. However, figure 3 shows that as temperature increases the difference in mobility in the two samples increases, showing that the filling per pore is different between the two samples. In the absence of atomistic modelling, we would suggest the simpler explanation based on a distribution of barriers that spans the same range in both samples. We propose that this arises from a shell layer of water at the pore surface progressing to a much greater mobility at the other surface of the water layer towards the centre of the pore, this range being independent of the layer thicknesses sampled in this experiment.

3. Summary

In this report, water confined in periodic mesoporous organosilicas with hydrophobic pore surface at two different hydration levels has been investigated with QENS. Although we cannot exclude subdiffusion, when analysed with a stretched exponential decay model the experimental data are consistent with inhomogeneous mobility. The inhomogeneity arises from shell layers of water molecules forming at the pore surface and progressively towards the centre of the pore. The derived EISFs indicate that a monolayer of water is bound to the surface of the pore and that the remainder diffuses in the pores with some evidence of a scale around 3.5 Å radius that we cannot attribute unambiguously. The effective diffusion constant is about a factor of 2 to 3 lower than bulk water at the same temperatures, particularly for the sample with lower hydration, which together show the effects of interactions with the pore surface. The similar values of diffusion constants of the current measurements to those of Vycor, silica nanopores and carbon nanotubes indicate that the property of the pore surface, hydrophilic or hydrophobic, does not play a major role in the dynamics of water confined in nano-scale structures. This also provides a verification of our initial analysis leading to a qualitative picture of the diffusion behaviour of water confined in porous silica. Deeper understanding will be obtained at a later stage by validating a molecular dynamics (MD) simulation against the experimental data, and then extracting the microscopic details of the diffusion process from the MD trajectories.

Acknowledgment

We acknowledge financial support from the Access to Major Research Facilities Programme which is a component of the international Science Linkages Programme established under the Australian Government's innovation statement, Backing Australia's Ability.

References

[1] N. Kallay: Interfacial Dynamics, CRC Press, 2000.
[2] A. Fouzri, R. Dorbez-Sridi and M. Oumezzine: Journal of Chemical Physics **116** (2002) 791.
[3] Y. Wang and S.L. Dong: Chinese Phys. Lett., **19** (2002) 711.
[4] J. C. Li, C. Burnham, A. I. Kolesnikov and R. S. Eccleston: Physical Review B **59** (1999) 9088.
[5] J. Qvist, H. Schober and B. Halle: J. Chem. Phys., **134** (2011) 144508.
[6] M. C. Bellisent-Funel, S. H. Chen, J. M. Zanotti: Phys. Rev. E**51** (1995) 4558.
[7] E. Mamontov, D. R. Cole, S. Dai, M. D. Pawel, C. D. Liang, T. Jenkins, G. Gasparovic, and E. Kintzel: Chem. Phys. **352** (2008) 3117.
[8] N. Floquet, J. P. Copulomb, G. Dufau, G. André, and R. Kahn: Phys. B**350** (2004) 265.
[9] S. Takahara, S. Kittaka, T. Mori, Y. Kuroda, T. Yamaguchi, M. C. Bellisent-Funel: Adsorption **11** (2005) 479.
[10] S. Takahara, N. Sumiyama, S. Kittaka, T. Yamaguchi, M. C. Bellisent-Funel: J. Phys. Chem. B**109** (2005) 11231.
[11] S. Mitra, R. Mukhopadhyay, I. Tsukushi, S. J. Ikeda: J. Phys.:Condens. Matter **13** (2001) 8455.
[12] S.H. Lee and P.J. Rossky: J. Chem. Phys. **100** (1994) 3334.
[13] S. H. Chen, P. Gallo, and M. C. Bellissent-Funel: in Non-Equilibrium Phenomena in Supercooled Fluids, Glasses and Amorphous Materials, edited by M. Giordano, D. L. Leporini, and M. P. Tosi (World Scientific, Singapore, 1996) p. 186.
[14] S. H. Chen, P. Gallo, F. Sciortino, and P. Tartaglia: in Supercooled Liquids: Advances and Novel Applications, edited by J. T. Fourkas, D. Kievelson, U. Mohanty, and K. A. Nelson, ACS Symposium Series No. 676 (ACS, Washington, DC,1997) p. 264.
[15] G. Hummer, J. C. Rasalaiah, and J. P. Noworyta: Nature **414** (2001) 188.
[16] X.- Q. Chu, A . I. Kolesnikov, A. P. Moravsky, V. Garcia-Sakai, and S.-H. Chen: Phys. Rev. E**76** (2007) 021505.
[17] S. M. Chathoth, E. Mamontov, A. I. Kolesnikov, Y. Gogotsi and D. J. Wesolowski: Euro. Phys. Lett. **95** (2011) 56001.
[18] E. Mamontov, C. J. Burnham, S.-H. Chen, A. P. Moravsky, C.-K. Loong, N. R. de Souza, and A. I. Kolesnikov: J. Chem. Phys. **124** (2006) 194703.
[19] D. Russo, R. K. Murarka, J. R. D. Copley and T. H. Gordon: J. Phys. Chem. B **109** (2005) 12966
[20] R. Bergman: J. Appl. Phys. **88** (2000) 1356.
[21] C.S. Kealley, A.V. Sokolova , G.J. Kearley , E. Kemner, M. Russina, A. Faraone, W.A. Hamilton, E.P. Gilbert: Biochimica et Biophysica Acta **1804** (2010) 34.
[22] S. H. Chen, C. Liao, F. Sciortino, P. Gallo, and P. Tartaglia: Phys. Rev. E**59** (1999) 6708.
[23] J.-M. Zanotti, M.-C. Bellissent-Funel, and S.-H. Chen: Phys. Rev. E**59** (1999) 3084.
[24] M. C. Bellissent-Funel, S. Longeville, J. M. Zanotti, and S. H. Chen: Phys. Rev. Lett. **85** (2000) 3645.
[25] S H Chen, Y Zhang, M Lagi, S H Chong, P Baglioni and F Mallamace: J. Phys.: Condens. Matter **21** (2009) 504102.
[26] Antonio Faraone, Li Liu, Chung-Yuan Mou, Pei-Chun Shih, John R. D. Copley and Sow-Hsin Chen: J. Chem. Phys. **119** (2003) 3963.
[27] F. Mansour, R. M. Dimeo, and H. Peemoeller: Phys. Rev. E**66** (2002) 041307.
[28] M. Holz, S. R. Heil and A. Sacco: Phys. Chem. Chem. Phys. **2**, (2000) 4740.
[29] M. C. Bellissent-Funel, S. H. Chen, and J.-M. Zanotti: Phys. Rev. E**51** (1995) 4558.